27/28th International Conference
ENGINEERING MECHANICS 2022
Milovy, Czech Republic, May 9 –12, 2022
Paper **#71**, pp. 249–252, doi: 10.21495/51-2-249

A QUICK CALIBRATION TOOL FOR CYCLIC PLASTICITY USING ANALYTICAL SOLUTION

Marek R.*, Parma S., Klepač V., Feigenbaum H. P.**

Abstract: *Calibrating a complex multi-parameter model on a large set of experimental data is extremely time-consuming. In this work, a closed-form solution of a multi-component Armstrong-Frederick model in uniaxial loading conditions is used as an efficient calibration tool. The intended application is large sets of experimental data for ratcheting.*

Keywords: Plasticity, Kinematic hardening, Armstrong-Frederick, Ratcheting, Calibration.

1. Introduction

In the world of plasticity modeling, ratcheting is the accumulation of plastic strain during stress-driven cyclic loading. This phenomenon is quite difficult to predict as small errors in each cycle accumulate to make large errors. Models to predict ratcheting have become more complex in attempts to improve predictions, see (Halama, 2008). While these models do show improvements, they are quite challenging to calibrate as they often include several material parameters. In this work, we devised an analytical solver for the purposes of study and calibration. Some previous results were published in (Parma et al., 2018), where analytical tools were used to calibrate a model that included yield surface distortion. The model in question is more manageable, an ordinary von Mises yield surface and a Multicomponent Armstrong-Frederick kinematic hardening rule with threshold modification according to Dafalias and Feigenbaum (2011). This has been used in various works with partial success on biaxial ratcheting predictions in (Welling et al., 2017) and in further numerical experiments in (Marek et al., 2022).

Employing the double dot product (:), the first three base components evolve according to the rule

$$\dot{\boldsymbol{\alpha}}_i = \langle\lambda\rangle\sqrt{\tfrac{2}{3}}c_i\left\{\sqrt{\tfrac{2}{3}}a_i^{\mathrm{S}}\mathbf{n} - \left[r_i\boldsymbol{\alpha}_i + (1-r_i)\,(\boldsymbol{\alpha}_i\!:\!\mathbf{n})\,\mathbf{n}\right]\right\}, \quad (i=1,2,3)\,, \tag{1}$$

with $r_i = \|\boldsymbol{\alpha}_i\|\,/a_i^{\mathrm{S}}$, while the fourth component, featuring a linear hardening part, is driven by

$$\dot{\boldsymbol{\alpha}}_4 = \langle\lambda\rangle\sqrt{\tfrac{2}{3}}c_4\left\{\sqrt{\tfrac{2}{3}}a_4^{\mathrm{S}}\mathbf{n} - \left[r_4\boldsymbol{\alpha}_4 + (1-r_4)\,(\boldsymbol{\alpha}_4\!:\!\mathbf{n})\,\mathbf{n}\right]\left\langle 1 - \sqrt{\tfrac{2}{3}}\frac{\bar{a}}{\|\boldsymbol{\alpha}_4\|}\right\rangle\right\}, \tag{2}$$

with $r_4 = \|\boldsymbol{\alpha}_4\|\,/\left(a_4^{\mathrm{S}} + \bar{a}\right)$. In the original paper, Dafalias and Feigenbaum (2011) defined the variable r_4 incorrectly. The weights r_i serve as a modification of a regular Armstrong-Frederick rule and affect multiaxial loading. The model is controlled by the rate parameters c_i and the saturation limits a_i^{S}. Parameter $\bar{a}$ represents the amplitude of the embedded linear hardening part, activated by the Macaulay brackets $\langle\,\rangle$. The linear part removes attraction towards zero backstress and, therefore, provides a way to limit ratcheting speed even in a non-symmetric cyclic loading. The asymptotic limits of the three base components are at

$$\left\|\boldsymbol{\alpha}_i^{\lim}\right\| = \sqrt{\tfrac{2}{3}}a_i^{\mathrm{S}}, \quad (i=1,2,3)\,, \tag{3}$$

* Ing. René Marek, Ph.D., Ing. Slavomír Parma, Ph.D., Ing. Vilém Klepač: Department D4 - Impact and Waves in Solids, Institute of Thermomechanics of the CAS, v. v. i., Dolejškova 1402/5; 182 00, Praha 8; CZ; {marek, parma, klepac}@it.cas.cz

** Heidi P. Feigenbaum, Ph.D.: Mechanical Engineering Department, Northern Arizona University, 15600 S. McConnell Dr. NAU, Flagstaff, AZ 86001-5600, USA; Heidi.Feigenbaum@nau.edu

while the fourth component evolves through its linear threshold at $\left\|\boldsymbol{\alpha}_4^{\mathrm{th}}\right\| = \sqrt{\frac{2}{3}}\bar{a}$ towards its asymptotic limit at

$$\left\|\boldsymbol{\alpha}_4^{\mathrm{lim}}\right\| = \sqrt{\tfrac{2}{3}}\left(a_4^{\mathrm{S}} + \bar{a}\right). \tag{4}$$

For the material used in this project, a three-component non-linear isotropic hardening rule was adopted as

$$\dot{k}_i = \langle\lambda\rangle\kappa_i\left(1 - \xi_i k_i\right), \quad (i = 1, 2, 3), \tag{5}$$

where κ_i represent rates of hardening and ξ_i represent inverted asymptotic limits. Variable k_1 is initiated as the initial yield stress k_0, while k_2 and k_3 start evolving from 0. All of them act in a sum as the radius of the yield surface. The model presumes associative flow rule defined as

$$\dot{\boldsymbol{\varepsilon}}_{\mathrm{p}} = \lambda\mathbf{n} \tag{6}$$

which decouples the actual value of yield function gradient from the model's behavior and strictly uses the unit outer normal $\|\mathbf{n}\| = 1$.

2. Analytical solution

The following solver provides the solution of a stress-, as well as strain-controlled uniaxial cyclic loading sequence. Axial stress σ_{x} or axial strain ε_{x} are expressed as functions of axial plastic strain $\varepsilon_{\mathrm{xp}}$. To reach the uniaxial stress solution, plastic strain has to be solved numerically. In the following code, deviatoric tensors are represented by their oriented norms.

2.1. Analytical solver

The analytical solver needs point of the last plastic reversal as input. This point is characterized by the set of backstress component norms α_i^0, the actual state of plastic strain $\varepsilon_{\mathrm{xp}}^0$, and the accumulated effective plastic strain $\varepsilon_{\mathrm{p}}^{\mathrm{cum0}}$. The active loading orientation is defined by $D \in \{-1, 1\}$. The algorithm checks the yield condition, and either returns the elastic solution, or proceeds to calculate the required plastic strain. If plastic reversal is encountered, the solver updates the referential point.

1. Evaluate radial stress: $S_{\mathrm{R}} = \sqrt{\frac{2}{3}}\sigma_{\mathrm{x}}^{\mathrm{trial}} - \sum_{i=1}^{4}\alpha_i \quad \vee \quad S_{\mathrm{R}} = \sqrt{\frac{2}{3}}\left(\varepsilon_{\mathrm{x}}^{\mathrm{trial}} - \varepsilon_{\mathrm{xp}}\right)E - \sum_{i=1}^{4}\alpha_i$
2. **if** $|S_{\mathrm{R}}| \leq \sqrt{\frac{2}{3}}\sum_{i=1}^{3}k_i$ **then** Return the elastic response: $\sigma_{\mathrm{x}} = \sigma_{\mathrm{x}}^{\mathrm{trial}} \quad \vee \quad \varepsilon_{\mathrm{x}} = \varepsilon_{\mathrm{x}}^{\mathrm{trial}}$

   else $D = \mathrm{sgn}\left(S_{\mathrm{R}}\right)$

   (a) Check for plastic reversal and update $\alpha^0, \varepsilon_{\mathrm{xp}}^0, \varepsilon_{\mathrm{p}}^{\mathrm{cum0}}$

   (b) Solve $R\left(\Delta\varepsilon_{\mathrm{xp}}\right) = 0$; $\quad \varepsilon_{\mathrm{p}}^{\mathrm{cum}} = \varepsilon_{\mathrm{p}}^{\mathrm{cum0}} + \Delta\varepsilon_{\mathrm{xp}}$; $\quad \varepsilon_{\mathrm{xp}} = \varepsilon_{\mathrm{xp}}^0 + D\cdot\Delta\varepsilon_{\mathrm{xp}}$; $\quad \varepsilon_{\mathrm{x}} = \sigma_{\mathrm{x}}/E + \varepsilon_{\mathrm{xp}}$

2.2. Stress residual $R\left(\Delta\varepsilon_{\mathrm{xp}}\right)$

Available tools were used to solve the root of the stress residual. A failure to secure the intermediate value theorem will occur if stress loading exceeds the ultimate strength.

1. $k_1 = \xi_1^{-1}\left[1 - \left(1 - \xi_1 k_0\right)\exp\left(-\sqrt{\frac{3}{2}}\kappa_1\xi_1\left(\varepsilon_{\mathrm{p}}^{\mathrm{cum0}} + \Delta\varepsilon_{\mathrm{xp}}\right)\right)\right]$
2. $k_i = \xi_i^{-1}\left[1 - \exp\left(-\sqrt{\frac{3}{2}}\kappa_i\xi_i\left(\varepsilon_{\mathrm{p}}^{\mathrm{cum0}} + \Delta\varepsilon_{\mathrm{xp}}\right)\right)\right],\ (i = 2, 3)$
3. $\alpha_i = \sqrt{\frac{2}{3}}D\cdot a_i^{\mathrm{S}} - \left(\sqrt{\frac{2}{3}}D\cdot a_i^{\mathrm{S}} - \alpha_i^0\right)\exp\left(-c_i\Delta\varepsilon_{\mathrm{xp}}\right),\ (i = 1, 2, 3)$; $\quad \alpha_4 \leftarrow D\cdot\alpha_4^0$; $\quad \Delta\varepsilon_{\mathrm{xp}}^{\mathrm{thr}} \leftarrow 0$;
4. **if** $\alpha_4 < -\sqrt{\frac{2}{3}}\bar{a}$ **then**

(a) $\Delta\varepsilon_{\mathrm{xp}}^{\mathrm{thr}} \leftarrow -c_4^{-1} \ln\left[a_4^{\mathrm{S}} / \left(a_4^{\mathrm{S}} - \bar{a} - \sqrt{\frac{3}{2}}\alpha_4\right)\right]$

(b) $\alpha_4 \leftarrow \sqrt{\frac{2}{3}}\left(a_4^{\mathrm{S}} - \bar{a}\right) - \left(\sqrt{\frac{2}{3}}\left(a_4^{\mathrm{S}} - \bar{a}\right) - \alpha_4\right) \exp\left(-c_4 \min\left\{\Delta\varepsilon_{\mathrm{xp}}, \Delta\varepsilon_{\mathrm{xp}}^{\mathrm{thr}}\right\}\right)$

(c) $\Delta\varepsilon_{\mathrm{xp}} \leftarrow \left\langle \Delta\varepsilon_{\mathrm{xp}} - \Delta\varepsilon_{\mathrm{xp}}^{\mathrm{thr}} \right\rangle$

5. **if** $\Delta\varepsilon_{\mathrm{xp}} > 0 \quad \wedge \quad \left(\Delta\varepsilon_{\mathrm{xp}}^{\mathrm{thr}} > 0 \ \vee \ \alpha_4 \leq \sqrt{\frac{2}{3}}\bar{a}\right)$ **then**

$$\Delta\varepsilon_{\mathrm{xp}}^{\mathrm{thr}} \leftarrow \frac{\bar{a} - \sqrt{\frac{3}{2}}\alpha_4}{c_4 a_4^{\mathrm{S}}}; \quad \alpha_4 \leftarrow \alpha_4 + \sqrt{\frac{2}{3}} c_4 a_4^{\mathrm{S}} \min\left\{\Delta\varepsilon_{\mathrm{xp}}, \Delta\varepsilon_{\mathrm{xp}}^{\mathrm{thr}}\right\}; \quad \Delta\varepsilon_{\mathrm{xp}} \leftarrow \left\langle \Delta\varepsilon_{\mathrm{xp}} - \Delta\varepsilon_{\mathrm{xp}}^{\mathrm{thr}} \right\rangle$$

6. **if** $\Delta\varepsilon_{\mathrm{xp}} > 0$ **then** $\alpha_4 \leftarrow \sqrt{\frac{2}{3}}\left(a_4^{\mathrm{S}} + \bar{a}\right) - \left(\sqrt{\frac{2}{3}}\left(a_4^{\mathrm{S}} + \bar{a}\right) - \alpha_4\right) \exp\left(-c_4 \Delta\varepsilon_{\mathrm{xp}}\right)$

7. $\alpha_4 \leftarrow D \cdot \alpha_4; \quad \sigma_{\mathrm{x}} = \sqrt{\frac{3}{2}} \sum_{i=1}^{4} \alpha_i + D \sum_{i=1}^{3} k_i$

8. $R = \sigma_{\mathrm{x}}^{\mathrm{trial}} - \sigma_{\mathrm{x}} \quad \vee \quad R = \left[\varepsilon_{\mathrm{x}}^{\mathrm{trial}} - \left(\varepsilon_{\mathrm{xp}}^{0} + D \cdot \Delta\varepsilon_{\mathrm{xp}}\right)\right] E - \sigma_{\mathrm{x}}$

3. Calibration strategy

Three cyclic experiments, performed by Nečemer et al. (2021), were selected for the calibration of the model. These tests use $\pm 1.25\%$, $\pm 1.0\%$ and $\pm 0.75\%$ total strain with 38, 57 and 189 loops, respectively. The material exhibited slow hardening, which called for the addition of the isotropic variables. The calibration procedure consists of several steps:

1. Measure the elastic modulus E. The Poisson's ratio is not relevant for uniaxial tests.
2. Choose the inverse size of the yield surface ξ_1 that is reached at the depletion of the initial isotropic softening. A plateau can be imitated by later counterbalancing the rate of isotropic softening κ_1 and initial kinematic hardening.
3. Variables k_2, k_3 will provide slow hardening during cyclic loading. Establish the two asymptotic functions by estimating hardening rates and saturation levels with parameters $\xi_2, \kappa_2, \xi_3, \kappa_3$.
4. Estimate c_i in a geometric sequence with c_4 positioned somewhere in the middle. Set equal saturation limits and refine c_1 to provide a good continuity for the transition between elastic and plastic behavior.
5. Use small value of $\bar{a}$ to limit ratcheting speeds for non-zero mean stress.
6. Establish weights to each data point according to the quality of the data and use the calibration tool to refine the calibration while initiating it from a whole set of partially randomized initial guesses.
7. Check results and refine weights given to each data point to suppress artefacts or eventual discrepancy of the experimental data and the available features of the model.

4. Results

For calibration, all points of reversal were used, as they define the experiment. Additional points were randomly spread within the loops to make 1900 data points in total. The acquired set of parameters is in Table 1. A few randomly selected loops and their simulations are plotted in Figure 1.

5. Discussion

The speed provided by the existence of closed-form solution is hugely beneficial and offers a promising way to come close to an optimal calibration of a model. Generally, the calibration process needs to be closely monitored, given that the error function on a complex model can be very chaotic and if not properly conditioned, the calibration process often slips into undesirable state. Our continuous push to amass large body of experiments on a low number of materials will enable us to test models under wide variety of conditions and search for new phenomena to address in modeling.

Tab. 1: Model calibration

E	ν	k_0	κ_1	ξ_1^{-1}	κ_2	ξ_2^{-1}	κ_3	ξ_3^{-1}
[MPa]	[−]	[MPa]	[MPa]	[MPa]	[MPa]	[MPa]	[MPa]	[MPa]
68266	-	109.2	53700	61	576.2	75.15	35.3	61.8
c_1	c_2	c_3	c_4	a_1^{S}	a_2^{S}	a_3^{S}	a_4^{S}	$\bar{a}$
[−]	[−]	[−]	[−]	[MPa]	[MPa]	[MPa]	[MPa]	[MPa]
1858	363.8	108.4	10.1	64.6	49.8	10.2	10	7.2

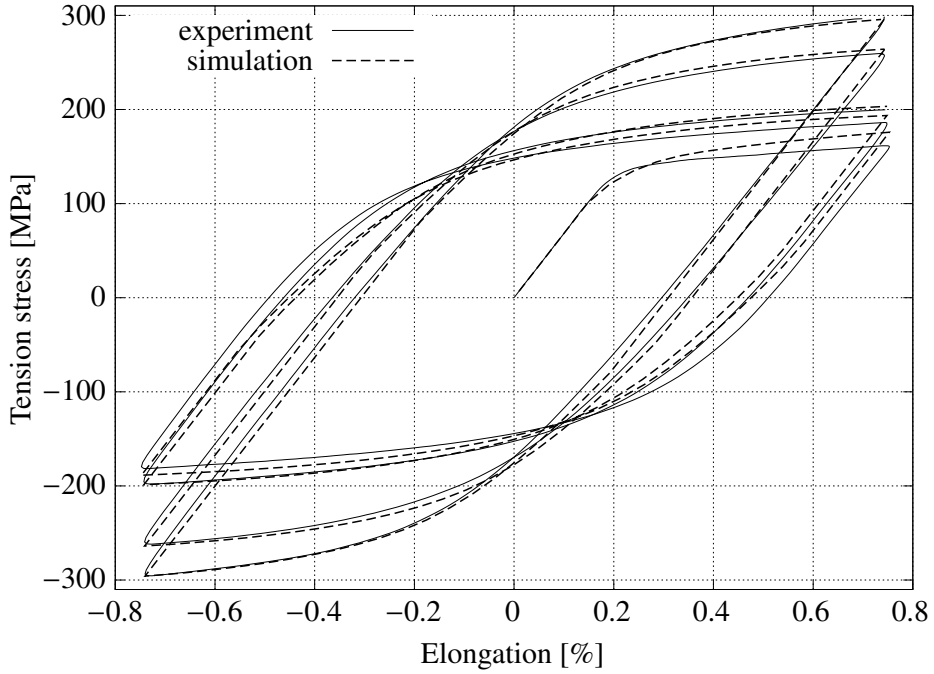

Fig. 1: A few randomly selected loops with comparison to the data from (Nečemer et al., 2021).

Acknowledgments

René Marek and Slavomír Parma acknowledge support by MEYS CR under grant project Centre of Excellence for Nonlinear Dynamic Behaviour of Advanced Materials in Engineering—CeNDYNMAT, grant No. CZ.02.1.01/0.0/0.0/15_003/0000493. René Marek acknowledges support by MEYS CR under grant No. LTA USA 18199. Heidi P. Feigenbaum acknowledges support by the US Army Research Laboratory and the US Army Research Office under Grant No. W911NF-19-1-0040. Vilém Klepač acknowledges support by the Institute of Thermomechanics of the Czech Academy of Sciences, grant No. RVO:61388998.

References

Dafalias, Y. F. and Feigenbaum, H. P. (2011), Biaxial ratchetting with novel variations of kinematic hardening. *International Journal of Plasticity*, Vol. 27, No. 4, pp. 479–491.

Halama, R. (2008), A modification of Abdelkarim-Ohno model for ratcheting simulations. Tehnički vjesnik, Vol. 15, No. 3, pp. 3–9.

Marek, R., Parma, S., and Feigenbaum, H. P. (2022), Distortional hardening cyclic plasticity—Experiments and modeling. In Jahed, H. and Roostaei, A. A., eds, *Cyclic Plasticity of Metals: Modeling Fundamentals and Applications*, Elsevier, pp. 175–225.

Nečemer, B., Zupanič, F., Gabriel, D., Tarquino, E.A., Šraml, M. and Glodež, S. (2021), Low cycle fatigue behaviour of ductile aluminium alloys using the inelastic energy approach. *Materials Science and Engineering: A*, Vol. 800, p. 140385.

Parma, S., Plešek, J., Marek, R., Hrubý, Z., Feigenbaum, H. P., and Dafalias, Y. F. (2018), Calibration of a simple directional distortional hardening model for metal plasticity. *Int. J. of Solids and Structures*, Vol. 143, pp. 113–124.

Welling, C. A., Marek, R., Feigenbaum, H. P., Dafalias, Y. F., Plešek, J., Hrubý, Z., and Parma, S. (2017), Numerical convergence in simulations of multiaxial ratcheting with directional distortional hardening. *International Journal of Solids and Structures*, Vol. 126–127, pp. 105–121.